Optical Vector Receiver Operating Near the Quantum Limit

V. A. Vilnrotter[1] and C.-W. Lau[1]

An optical receiver concept for binary signals with performance approaching the quantum limit at low average-signal energies is developed and analyzed. A conditionally nulling receiver that reaches the quantum limit in the absence of background photons has been devised by Dolinar. However, this receiver requires ideal optical combining and complicated real-time shaping of the local field; hence, it tends to be difficult to implement at high data rates. A simpler nulling receiver that approaches the quantum limit without complex optical processing, suitable for high-rate operation, had been suggested earlier by Kennedy. Here we formulate a vector receiver concept that incorporates the Kennedy receiver with a physical beamsplitter, but it also utilizes the reflected signal component to improve signal detection. It is found that augmenting the Kennedy receiver with classical coherent detection at the auxiliary beamsplitter output, and optimally processing the vector observations, always improves on the performance of the Kennedy receiver alone, significantly so at low average-photon rates. This is precisely the region of operation where modern codes approach channel capacity. It is also shown that the addition of background radiation has little effect on the performance of the coherent receiver component, suggesting a viable approach for near-quantum-limited performance in high background environments.

I. Introduction

Free-space optical communications enables high data rates with modest power levels and relatively small optical apertures, due primarily to the narrow beam widths that can be generated at optical frequencies. Another advantage of optical communication is that, due to the high energy of photons in the optical regime, energy detection becomes a viable option that can be used to discriminate between individual photons. Thus, photon-counting techniques have been used to overcome thermal noise in the detection electronics, leading to shot-noise-limited performance, where the only uncertainty is the inherent quantum-mechanical randomness in the weak optical fields. On the other hand, coherent detection of optical signals relies on the addition of a strong local optical field to generate a large cross-term between the received and local fields which, when detected using a suitable optical energy detector, also can overcome thermal noise and achieve shot-noise-limited performance.

---

[1] Communications Architectures and Research Section.

The research described in this publication was carried out by the Jet Propulsion Laboratory, California Institute of Technology, under a contract with the National Aeronautics and Space Administration.

In the following sections, the structure of a practical receiver for optical signals employing both photon-counting and coherent detection principles will be described and shown to approach the quantum limit in operating regions of interest. A complete description of the quantum and classical receiver structures is facilitated through the use of coherent states, which are defined in Section II. A vector receiver concept designed to approach the quantum limit is described in Section III, followed by the derivation of the detection algorithm based on maximum-likelihood principles and an analysis of receiver performance in Section IV. Numerical results are presented in Section V, including a discussion of vector receiver performance in the presence of interfering photons and a preliminary evaluation of the impact of modern codes on vector receiver performance.

II. Coherent-State Representation of Optical Signals

It has long been known that coherent states of the kind generated by lasers operating above threshold retain their basic properties even when suffering great losses, as usually occurs with long-range free-space communications, and especially in the emerging field of deep-space optical communications. This property of coherent states facilitates the design of optical communications systems, since the detection algorithm can be derived independently of the operating range. For this reason, optical communications systems based on laser transmitters generating coherent-state signals and conventional optical receiver components are attractive for long-range communications applications. A thorough description and performance analysis of optical communications systems generally requires a formulation of the problem in terms of coherent states. A brief description of coherent states, along with some of their most important properties, follows.

A coherent-state $|\alpha\rangle$, representing a single mode of an optical field, can be represented in terms of a superposition of orthonormal number states $|n\rangle$ as in [1]:

$$|\alpha\rangle = e^{-(1/2)|\alpha|^2} \sum_{n=0}^{\infty} \frac{\alpha^n}{(n\,!)^{1/2}}\, |n\rangle \tag{1}$$

Each number eigenstate $|n\rangle$ contains n photons, and hence the probability of obtaining exactly n photons as the outcome of an experiment is given by the Poisson distribution:

$$P(n) = |\langle \alpha | n \rangle|^2 = e^{-|\alpha|^2} \frac{|\alpha|^{2n}}{n\,!} \tag{2}$$

where $|\alpha|^2$ is the average number of photons in the coherent state. Coherent states are not orthogonal, as can be seen by considering the overlap between two arbitrary coherent states, $|\alpha_1\rangle$ and $|\alpha_2\rangle$. Orthogonality requires that the overlap vanish altogether; however, for coherent states, the squared magnitude of the overlap is not zero but instead is given by

$$|\langle \alpha_1 | \alpha_2 \rangle|^2 = \left| e^{-(|\alpha_1|^2+|\alpha_2|^2)/2} \sum_n \sum_m \frac{\alpha_1^n}{\sqrt{n\,!}} \frac{(\alpha_2^*)^m}{\sqrt{m\,!}} \langle n | m \rangle \right|^2 = \left| e^{-(|\alpha_1|^2+|\alpha_2|^2-2\alpha_1\alpha_2^*)/2} \right|^2 = e^{-|\alpha_1-\alpha_2|^2} \tag{3}$$

where we made use of the orthogonality of the number states to simplify the expression. Equation (3) demonstrates that there is always some overlap between coherent states. In the context of optical communications, this implies that coherent states cannot be distinguished without error, even when individual photons can be observed without any interfering thermal noise.

III. Vector Receiver Structure

Optical receivers that approach the quantum limit [2,3] and actually attain the quantum limit under ideal conditions [4] have been developed using conceptually realizable quasi-physical components and techniques. These receivers were designed primarily for the noiseless channel, and they utilize idealized (lossless) optical components to coherently combine the optical fields, together with photon-counting detection, and wideband processing and control in an optical feedback configuration to achieve optimum performance. Here we search for simpler receiver structures employing realistic optical components readily available in the laboratory, and we investigate their ability to approach quantum-limited performance under realistic deep-space operating conditions.

A reasonable starting point is a version of the near-optimum receiver for the reception of binary phase-shift keyed (BPSK) signals, but considered in a more general framework that includes realistic modeling of key optical components. The near-optimum receiver adds to the received field a local field of the same amplitude as the signal, with phase perfectly matched to the received phase under one of two hypotheses, H_0 or H_1 (with no loss in generality, we assume the phase of the local field corresponds to that of the received field, given H_1). With perfect amplitude and phase matching, this implies that the amplitude of the received signal field is doubled under H_1, but that the received field is effectively canceled under H_0. We extend this original idealized construction presented in [2] by including a more realistic beam-splitter model with non-zero reflection, to which we add a local field of the correct amplitude to ensure that the constraints of the Kennedy receiver are met for any value of beam-splitter reflectivity. This construction implies that there will be a component due to the reflected signal and the transmitted local field that will also contain information about the received hypothesis and that, therefore, should not be ignored. The following investigation is based on the generalized block diagram of Fig. 1, in which both beam-splitter ports are identified and the relevant signal and local field parameters are defined. The question we wish to answer is the following: Is it possible to improve upon the performance of the original Kennedy receiver by observing both output ports of a realistic beam splitter, when operating under realistic conditions including finite local oscillator power, realistic beam-splitter reflectivity, and interfering background radiation?

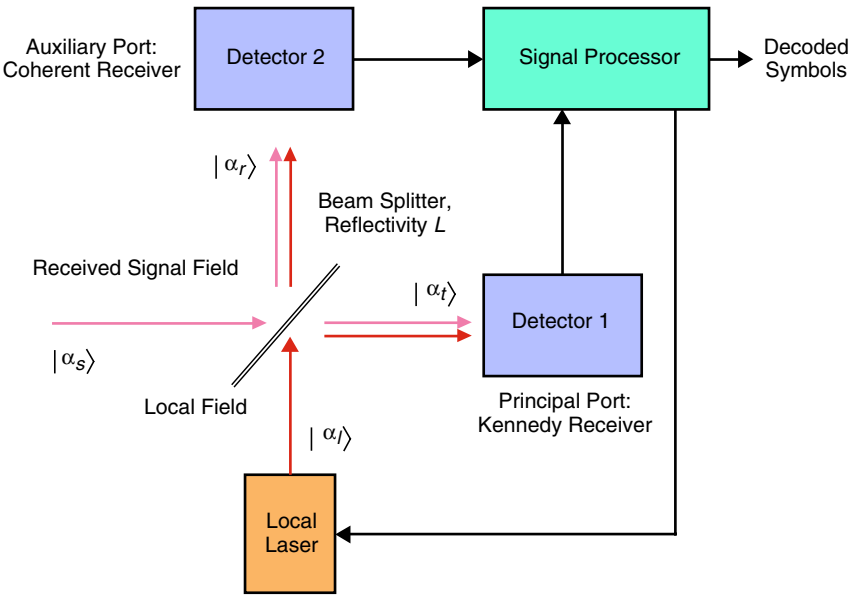

Fig. 1. Conceptual block diagram of the vector receiver; bit decisions are based on both beam-splitter outputs.

The received optical fields are combined with a locally generated optical field of the same wavelength and precisely controlled amplitude and optical phase on the surface of a beam splitter, whose reflectivity L can take any value between zero and one: $0 \leq L \leq 1$ (here we take the view that reflectivity is a loss to the principal port). Combinations of the received and local fields appear at both outputs of the beam splitter and are detected by photon counters or other appropriate optical detectors. Since our investigations are motivated by the receiver structure originally proposed by Kennedy [2], which employs ideal combining optics and photon counters, a photon-counting detector was assigned to the principal output, or port, of the beam splitter (here "principal output" is defined as containing most of the received signal field in the limit of vanishingly small reflectivity). The secondary output is not constrained, allowing the use of any appropriate detector or detection technique. As originally reported, the Kennedy and Dolinar receivers observe only the principal port, relying on arbitrarily small reflectivity and hence arbitrarily large local laser power in order to achieve the required field matching; however, this approach is not always feasible since practical local laser power is limited, but more importantly because scattering from imperfections or dust on the optical surfaces becomes intense as the laser power is increased, resulting in undesirable interfering photons. The results of a previous analysis of near-optimum receiver performance in the presence of background and random phase errors reported in [3], along with more recent simulations of the optimum receiver,[2] were used to investigate and compare receiver performance in the presence of background photons. As shown in Fig. 2, the addition of even a single background photon to the received signal during a bit interval results in significant performance degradation in both receivers.

As a first step to extending the zero-reflectivity single-output analyses reported in [2,4], likelihood ratios were derived for the practical two-port scenario described in Fig. 1, where the beam-splitter reflectivity is allowed to vary and, hence, so is the required local laser power.

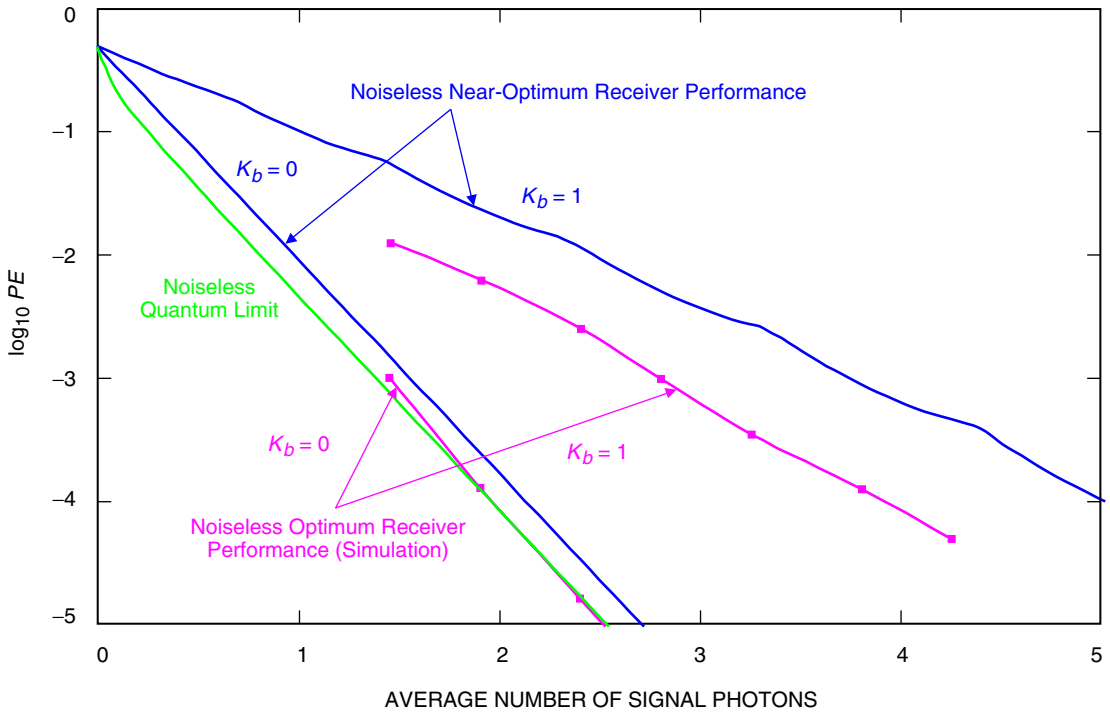

Fig. 2. Performance comparison of optimum and near-optimum noiseless receivers, with background.

[2] Discussed in V. Vilnrotter, H. Mabuchi, C.-W. Lau, S. J. Dolinar, and M. Munoz-Fernandez, *Quantum Detection of Classical Signals*, DRDF Interim Report (internal document), Jet Propulsion Laboratory, Pasadena, California, October 15, 2004.

When the inputs to the beam splitter are coherent states, so are the outputs; only the amplitudes of the coherent states are affected. The resulting optical fields at the "reflected" and "transmitted" outputs (with respect to the received signal field) can be determined from the following matrix equation [5]:

$$\begin{pmatrix} |\alpha_r\rangle \\ |\alpha_t\rangle \end{pmatrix} = \begin{pmatrix} \sqrt{L} & \sqrt{1-L} \\ \sqrt{1-L} & -\sqrt{L} \end{pmatrix} \begin{pmatrix} |\alpha_s\rangle \\ |\alpha_l\rangle \end{pmatrix} \tag{4}$$

resulting in the scalar components

$$\begin{aligned} |\alpha_r\rangle &= |\sqrt{L}\alpha_s + \sqrt{1-L}\alpha_l\rangle \\ |\alpha_t\rangle &= |\sqrt{1-L}\alpha_s - \sqrt{L}\alpha_l\rangle \end{aligned} \tag{5}$$

When the constraint of the Kennedy receiver is imposed on the local field (to cancel or reinforce the received field), the coherent state representing the local field required to cancel the transmitted portion of the received field becomes $|\alpha_l\rangle = |\sqrt{1-L}\alpha_s/\sqrt{L}\rangle$. Under the two hypotheses H_0 and H_1, this results in the following transmitted coherent states:

$$\begin{aligned} H_0: &\quad |\alpha_t\rangle = |0\rangle \\ H_1: &\quad |\alpha_t\rangle = |-2\sqrt{1-L}\alpha_s\rangle \end{aligned} \tag{6a}$$

At the same time, the reflected components at the auxiliary port become

$$\begin{aligned} H_0: &\quad |\alpha_r\rangle = |\alpha_s/\sqrt{L}\,\rangle \\ H_1: &\quad |\alpha_r\rangle = |\,(1-2L)\,\alpha_s/\sqrt{L}\,\rangle \end{aligned} \tag{6b}$$

The resulting transmitted fields give rise to coherent states with an average number of photons proportional to the squared magnitude of the field amplitudes. These combined field amplitudes give rise to the following conditional densities of photons, k, for the transmitted field observed at the principal port:

$$\begin{aligned} \lim_{\varepsilon\to 0} p\,(k|H_0,\varepsilon) &= |\varepsilon|^{2k} \exp\left[-|\varepsilon|^2\right]/k! = \delta(k) \\ p\,(k|H_1) &= \left[4(1-L)|\alpha|^2\right]^k \exp\left[-4(1-L)|\alpha|^2\right]/k! \end{aligned} \tag{7a}$$

where

$$\delta(k) = \begin{cases} 1, & k=0 \\ 0, & k \geq 1 \end{cases}$$

Although the received field under hypothesis zero is completely canceled at the principal port, to facilitate the analysis we prefer to further condition on a small residual field, giving rise to an average photon count

of ε; then let ε approach zero. Similarly, the conditional densities of photons under the two hypotheses at the auxiliary port become

$$\begin{aligned} p(k|H_0) &= |\alpha_s/\sqrt{L}\,|^{2k} \exp\left[-|\alpha_s|^2/L\right]/k! \\ p(k|H_1) &= |(1-2L)\alpha_s/\sqrt{L}\,|^{2k} \exp\left[-|(1-2L)\alpha_s|^2/L\right]/k! \end{aligned} \tag{7b}$$

Let us pause briefly to examine the key difference between the observed processes at the two receiver ports. Consider the case where the average number of photons in the received coherent state under either hypothesis is 1 photon, and the reflectivity is one percent, or $L = 0.01$. This represents a realistic region of operation of modern receivers, especially when the binary symbols are encoded for enhanced operation near channel capacity. At the principal port, the receiver attempts to distinguish between complete absence of a signal (zero photons on the average) and an average value of $4 \times 0.99 = 3.96$ photons; the probability of an erasure with this scheme is $e^{-3.96} = 0.019$, which leads to an average error probability of 0.0095 (after tossing a fair coin to resolve the ambiguity, according to the maximum-likelihood detection strategy). This error probability is within a factor of two of the quantum limit; hence, we may conclude that photon counting at the principal port leads to accurate detection under these conditions.

At the auxiliary port, however, the receiver attempts to distinguish between a Poisson random variable of average value 100 under hypothesis zero and of average value 96.04 under hypothesis one. Since the average values under both hypotheses are approximately 100 during each bit interval, photon counting becomes impractical at high data rates due to the high currents generated within the detector circuits, often leading to saturation or other losses in practical systems. Therefore, we propose the following detection scheme at the auxiliary port: Add an unconstrained but strong local field to the reflected field components, in phase with the constrained local field impinging on the beam splitter as described above, and then detect the resulting sum field using a simple unity-gain detector. Designating this second local field over each bit interval as $|\alpha_{l2}\rangle$, the average number of photons observed by the auxiliary detector under the two hypotheses becomes

$$\begin{aligned} H_0: &\quad \left(\alpha_{l2} + \alpha_s/\sqrt{L}\right)^2 = \alpha_{l2}^2 + \frac{2\alpha_{l2}\alpha_s}{\sqrt{L}} + \frac{\alpha_s^2}{\sqrt{L}} \cong \alpha_{l2}^2 + \frac{2\alpha_{l2}\alpha_s}{L} \\ H_1: &\quad \left(\alpha_{l2} + (1-2L)\alpha_s/\sqrt{L}\right)^2 = \alpha_{l2}^2 + \frac{2(1-2L)\alpha_{l2}\alpha_s}{\sqrt{L}} + \frac{(1-2L)^2\alpha_s^2}{L} \cong \alpha_{l2}^2 + \frac{2(1-2L)\alpha_{l2}\alpha_s}{\sqrt{L}} \end{aligned} \tag{8}$$

where we made use of the fact that $\alpha_s \ll \alpha_{l2}$. Because of the strong local oscillator field generated at the auxiliary port, it is customary to view the random processes under the two hypotheses as Gaussian, with mean values given by Eq. (8). Within the framework of the above assumptions, the detection problem is equivalent to deciding on the basis of the Gaussian conditional densities:

$$\begin{aligned} p\,(x|H_0) &= \exp\left[-\frac{1}{2}\left(x - 2\sqrt{L}|\alpha|\right)^2\right]/\sqrt{2\pi} \\ p\,(x|H_1) &= \exp\left[-\frac{1}{2}\left(x + 2\sqrt{L}|\alpha|\right)^2\right]/\sqrt{2\pi} \end{aligned} \tag{9}$$

where x is a continuous random variable proportional to the electric current generated by the detector in response to the intensity distribution due to the sum of a strong local field plus the signal field

over the detector's active surface. Since the detectors are observing two different beam-splitter outputs, the random processes generated at the detector outputs are independent, as are the random variables representing the integer-valued photon counts at the principal port and the continuous observables at the auxiliary port.

IV. Maximum-Likelihood Detection and Receiver Performance

Since the statistics of the observed processes at the two ports are independent, the joint probability of the two-component observation vector can be expressed as the product of the individual conditional densities. Therefore, the maximum-likelihood detection strategy is to compute the likelihoods on both sides of the inequality in Eq. (10) and select the hypothesis corresponding to the largest:

$$|\varepsilon|^{2k}\exp\left[-|\varepsilon|^2\right]\exp\left[-\frac{1}{2}\left(x-2\sqrt{L}|\alpha|\right)^2\right]\underset{H_1}{\overset{H_0}{\gtrless}}\left[2\sqrt{(1-L)}|\alpha|\right]^{2k}\exp\left[-4(1-L)|\alpha|^2\right]$$

$$\times\exp\left[-\frac{1}{2}\left(x+2\sqrt{L}|\alpha|\right)^2\right] \tag{10}$$

Recalling that the logarithm is a monotone increasing function of its argument, we can take the natural log of Eq. (10) to reduce the computational complexity:

$$k\ln|\varepsilon|^2-|\varepsilon|^2-\frac{1}{2}\left(x-2\sqrt{L}|\alpha|\right)^2\underset{H_1}{\overset{H_0}{\gtrless}}k\ln\left[2\sqrt{(1-L)}|\alpha|\right]^2-4(1-L)|\alpha|^2-\frac{1}{2}\left(x+2\sqrt{L}|\alpha|\right)^2 \tag{11}$$

Rearranging and simplifying yields

$$k\ln\left(|\varepsilon|/2|\alpha|\sqrt{1-L}\right)\underset{H_1}{\overset{H_0}{\gtrless}}-2x|\alpha|\sqrt{L}+\frac{1}{2}|\varepsilon|^2-2|\alpha|^2(1-L) \tag{12}$$

For any $\varepsilon>0$, there are two cases to consider: $k=0$ and $k\geq 1$. When $k=0$, the test reduces to

$$x\underset{H_1}{\overset{H_0}{\gtrless}}\frac{|\varepsilon|^2}{2|\alpha|\sqrt{L}}-\frac{|\alpha|\,(1-L)}{\sqrt{L}}\underset{\varepsilon\to 0}{=}-\frac{|\alpha|\,(1-L)}{\sqrt{L}}\equiv\eta \tag{13}$$

When $k\geq 1$, hypothesis H_1 is chosen as $\varepsilon\to 0$, because the logarithm on the left-hand side approaches $-\infty$ as $\varepsilon\to 0$; therefore, the right-hand side is always greater than the left-hand side, regardless of the value of x. Next we determine the average probability of error for the vector receiver when the maximum-likelihood detection algorithm is applied.

The average error probability $P(E)$ can be computed by first determining the average probability of correct detection, $P(C)$, and subtracting it from one: $P(E)=1-P(C)$. Next, we write the average probability of correct detection as the average of the conditional probabilities, averaged over the a priori probabilities: $P(C)=P(C|H_0)P(H_0)+P(C|H_1)P(H_1)$. Each conditional probability can be further decomposed according to the observation of any photons whatsoever at the principal port, and then averaged; for ML detection, the relevant photon counts are $k=0$ and $k\geq 1$. Hence, $P(C|H_0)=$

$P(C|H_0, k=0)P(k=0) + P(C|H_0, k\geq 1)P(k\geq 1)$, and similarly for $P(C|H_1)$. Recalling that $P(k=0) = \exp[-4|\alpha|^2(1-L)$ and $P(k\geq 1) = 1 - \exp[-4|\alpha|^2(1-L)$, the probability of correct detection can be expressed as

$$P(C) = \frac{1}{2}\left\{\left(1 - e^{-4|\alpha|^2(1-L)}\right)\right.$$

$$\left. + (2\pi)^{-1/2}\int_{-\eta}^{\infty} \exp\left[-\left(x - 2\sqrt{L}|\alpha|\right)^2/2\right] dx + e^{-4|\alpha|^2(1-L)}\int_{-\infty}^{-\eta} \exp\left[-\left(x + 2\sqrt{L}|\alpha|\right)^2/2\right] dx\right\} \tag{14}$$

The error probability of the vector receiver can be expressed in terms of the familiar error function $Q(y) = \int_y^{\infty} dx \exp[-z^2/2]/\sqrt{2\pi}$ as

$$P(E) = 1 - P(C) = \frac{1}{2}Q\left(|\alpha|(1+L)/\sqrt{L}\right) + \frac{1}{2}\exp\left[-4|\alpha|^2(1-L)\right]\left\{1 - Q\left(|\alpha|(1-3L)/\sqrt{L}\right)\right\} \tag{15}$$

In the following section, we will evaluate the performance of the vector receiver as a function of the beam-splitter reflectivity L for a given signal strength, and also as a function of the signal strength with optimized reflectivity. Finally, the impact of coding on vector receiver performance will be discussed.

V. Numerical Evaluation of Vector Receiver Performance

The performance of the vector receiver was first evaluated as a function of the beam-splitter reflectivity L, for several values of average received signal photons, $|\alpha|^2$. The results indicate a strong dependence on both L and $|\alpha|^2$, as illustrated in Figs. 3(a) and 3(b), which show the average probability of error as a function of L computed according to Eq. (15) at two different signal energies, namely, $|\alpha|^2 = 1$ in Fig. 3(a) and $|\alpha|^2 = 0.25$ in Fig. 3(b). In addition, two bounds are also shown, namely, the lossless quantum limit (that is, the quantum limit corresponding to the total signal energy) and the error probability of the lossy near-optimum receiver. The lossless quantum-optimum receiver achieves $P(E) = (1/2)[1 - \sqrt{1 - \exp(-4|\alpha|^2)}$, as shown in [5,6], which evaluates to approximately 0.0046 at an average rate of 1 photon, and to 0.35 at an average rate of 0.25 photons per symbol. Note that the error probability of the vector receiver is always lower than that of the lossy near-optimum receiver, as expected, since additional information about the received signal is obtained at the auxiliary port and used in an optimum manner. As the beam-splitter reflectivity approaches zero (or as the signal loss to the principal port approaches zero), the performances of the vector and near-optimum receivers coincide; however, operation in this regime requires infinite local laser power.

In Fig. 3(a), the error probability first increases as the reflectivity is increased from zero, following the performance of the near-optimum receiver, and then reverses direction and begins to decrease as the reflectivity approaches one. However, performance is best near zero reflectivity for this "high signal energy" case, and the same behavior is observed at even higher signal levels. This suggests that in this regime the reflectivity should be minimized and at the same time local laser power increased as required, in accordance with the original premise of the near-optimum receiver.

The behavior of the vector receiver changes substantially at low signal energies, as shown by the performance curves of Fig. 3(b). In this region, the performance of the near-optimum receiver again degrades with increasing loss, as expected; however, the performance of the vector receiver improves as the reflectivity increases, reaching a value close to the quantum limit as the reflectivity approaches one. In this regime of low signal energies, high reflectivities yield best performance.

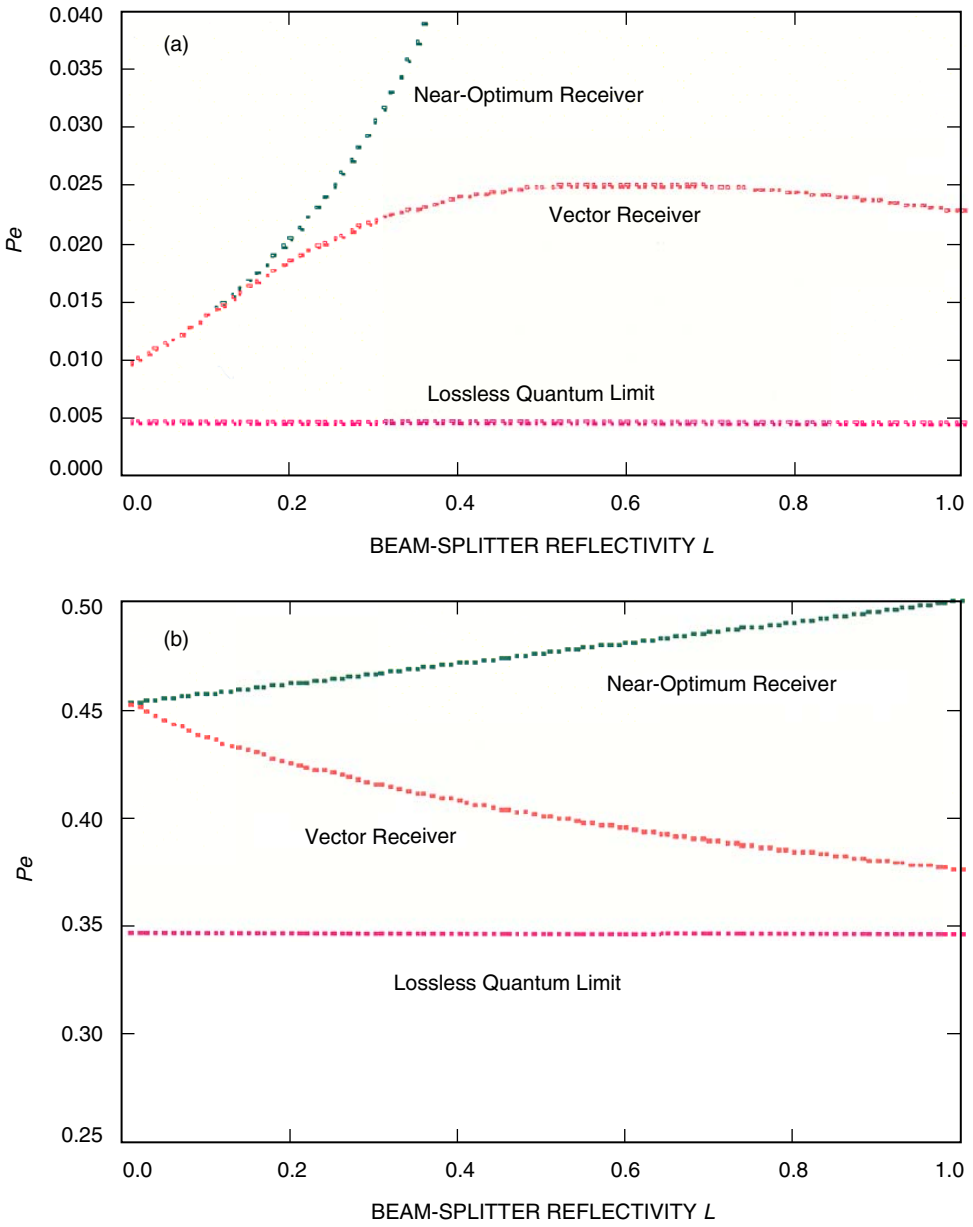

Fig. 3. Error probability of vector and near-optimum receivers as a function of reflectivity: (a) $|\alpha|^2 = 0.25$ and (b) $|\alpha|^2 = 1$.

The performance of the two-port receiver as a function of the average number of signal photons per symbol, $|\alpha|^2$, with reflectivity optimized at each value of $|\alpha|^2$, is shown in Fig. 4. Note that for $|\alpha|^2$ greater than about 0.4 photons per symbol the performance of the optimized vector receiver follows that of the lossless near-optimum receiver but always improves on the near-optimum receiver when beam-splitter losses are taken into account. However, for $|\alpha|^2 < 0.4$ photons, the vector receiver significantly outperforms the lossless near-optimum receiver, approaching the quantum bound as the average number of signal photons decreases. These results are applicable to conditions when non-signal photons due to background radiation or scattering of the strong local oscillator fields from the beam-splitter surface can be neglected. In general, the performance of the vector receiver can be approximated by the performance of the lossless near-optimum receiver alone when $|\alpha|^2 > 0.4$, and by the performance of the coherent

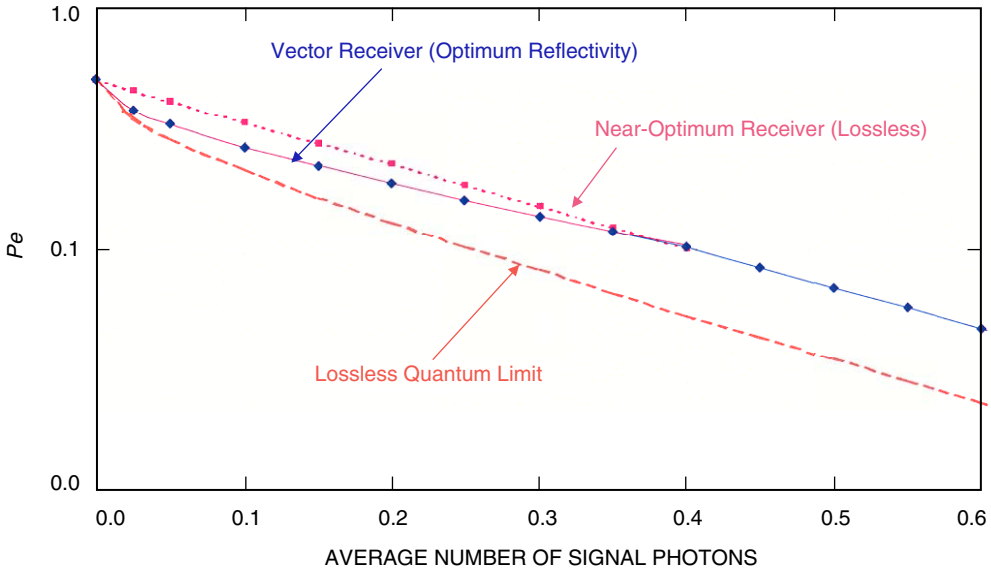

Fig. 4. Average (uncoded) bit-error probability of the vector receiver, compared with the quantum limit.

receiver alone when $0 < |\alpha|^2 < 0.4$. These approximations do not hold when significant amounts of interfering background or other non-signal photons are introduced into the system.

When more realistic background reception conditions typical of the optical free-space channel are taken into account, the performances of the near-optimum and quantum-optimum receivers degrade significantly, as demonstrated earlier in Fig. 2. An upper bound on the error probability of the vector receiver in the presence of background can be obtained by evaluating the performances of the two receiver components separately, and taking the lower envelope. Note that we have not derived the ML vector receiver structure in the presence of noise, but merely evaluated the performance of its two components.

In order to evaluate the performance of the vector receiver components under conditions of moderate background photons, the maximum-likelihood detection threshold was employed for the near-optimum receiver as derived in [2]. For the coherent detection algorithm at the auxiliary port, the signal-to-noise ratio was modified to account for strong background, replacing $|\alpha|^2$ in the argument of the Q-function with $|\alpha|^2/(1+2[\eta/h\nu]N_{0b})$ as described in [6], where N_{0b} is the spectral level of the background radiation, η is the detector's quantum efficiency, and h is Planck's constant. Recalling that the average number of background photons for multimode background radiation is given by $K_b = 2[\eta/h\nu]N_{0b}BT$, where B is the bandwidth of the optical predetection filter and T is the symbol duration, it follows that $2(\eta/h\nu)N_{0b} = K_b/BT$. Therefore, if we assume that there are an average of $K_b = 1$ multimode background photons per symbol, and that a 1-angstrom predetection filter was employed at a wavelength of 1 micrometer, then with 1-nanosecond symbol duration we find that $BT \cong 30$; hence, $2(\eta/h\nu)N_{0b} = K_b/BT \cong 1/30$ in our example.

The performances of the two vector receiver components, the near-optimum receiver and the coherent receiver, are shown in Fig. 5 in the presence of background noise of average value equal to one photon per symbol. For comparison, the performance of the optimum quantum receiver for BPSK symbols in the presence of background is also shown, computed two different ways: the truncated density-matrix eigenvalue solution originally developed in [6] and the more recent "rotation algorithm" solution described in [1,7]. Note that both approaches are approximate but yield nearly identical solutions in this case (however, the eigenvalue solution in [6] applies only to binary signals in noise, whereas the rotation algorithm can be applied to higher dimensional signal sets as well, when observed in the presence of noise, as described in [8]). The noiseless quantum limit is also included in Fig. 5 for completeness.

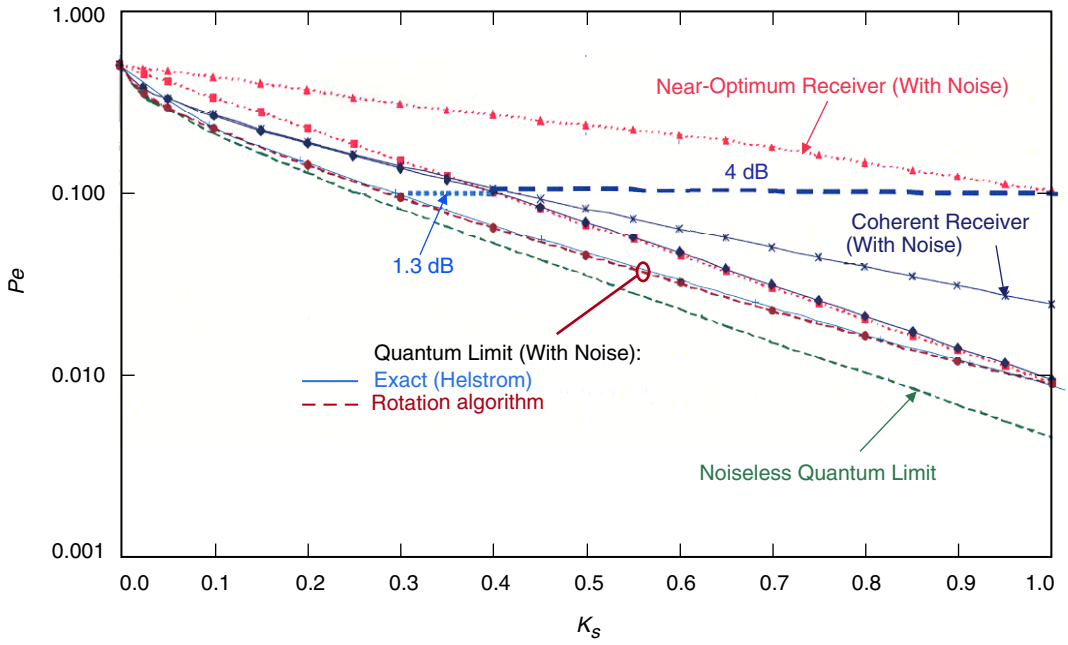

Fig. 5. Comparison of the near-optimum, optimum, and vector receivers, uncoded error probability, with and without background.

The performance of the coherent receiver is hardly affected by background photons, since these are not phase coherent with the signal and, therefore, contribute only slightly to the variance of the Gaussian observables. However, the near-optimum receiver suffers significant performance degradation when background (or other interfering) photons enter the receiver along with the signal, since it responds to photon energy regardless of phase; at an uncoded error probability of 0.1, the near-optimum receiver performs approximately 4-dB worse than the coherent receiver in Fig. 5. At the same uncoded error probability, the coherent receiver is within 1.3 dB of the quantum limit for detecting BPSK signals in the presence of noise.

It is interesting to note that, for the noiseless case, the crossover from the near-optimum receiver to the coherent receiver occurs for bit-error rates of 0.1 or greater, which is precisely the region of interest for coding, since it is in the low-photon region where the capacity of the channel can be approached by powerful codes such as low-density parity check (LDPC) and turbo codes that employ efficient iterative techniques. Coded performance of the vector receiver has been investigated near the crossover point of $|\alpha|^2 = 0.4$, for both the noiseless and noisy reception cases, and some examples are presented in Fig. 6, where we let $E_s/N_0(\text{dB}) = 10\log(|\alpha|^2/(1 + 1/30)$, in accordance with the noise spectral level defined above.

It can be seen that, even at a relatively high uncoded bit-error probability of 0.2, corresponding to $|\alpha|^2 = 0.15$ photons on the average, coded error probabilities of 10^{-3} or lower can be attained through the use of rate 1/4, length 8920 turbo codes. To achieve the same performance, the near-optimum receiver would require 4.6-dB greater signal energy when operating in the presence of moderate background noise. Note that greatly improved receiver performance can be attained by the use of low-rate codes even when the uncoded bit-error probability is greater than 0.1, which is precisely the region where the vector receiver closely approaches the noiseless quantum bound; however, significant performance improvements can also be realized with higher rate, hence less complex, codes when greater signal energies are available.

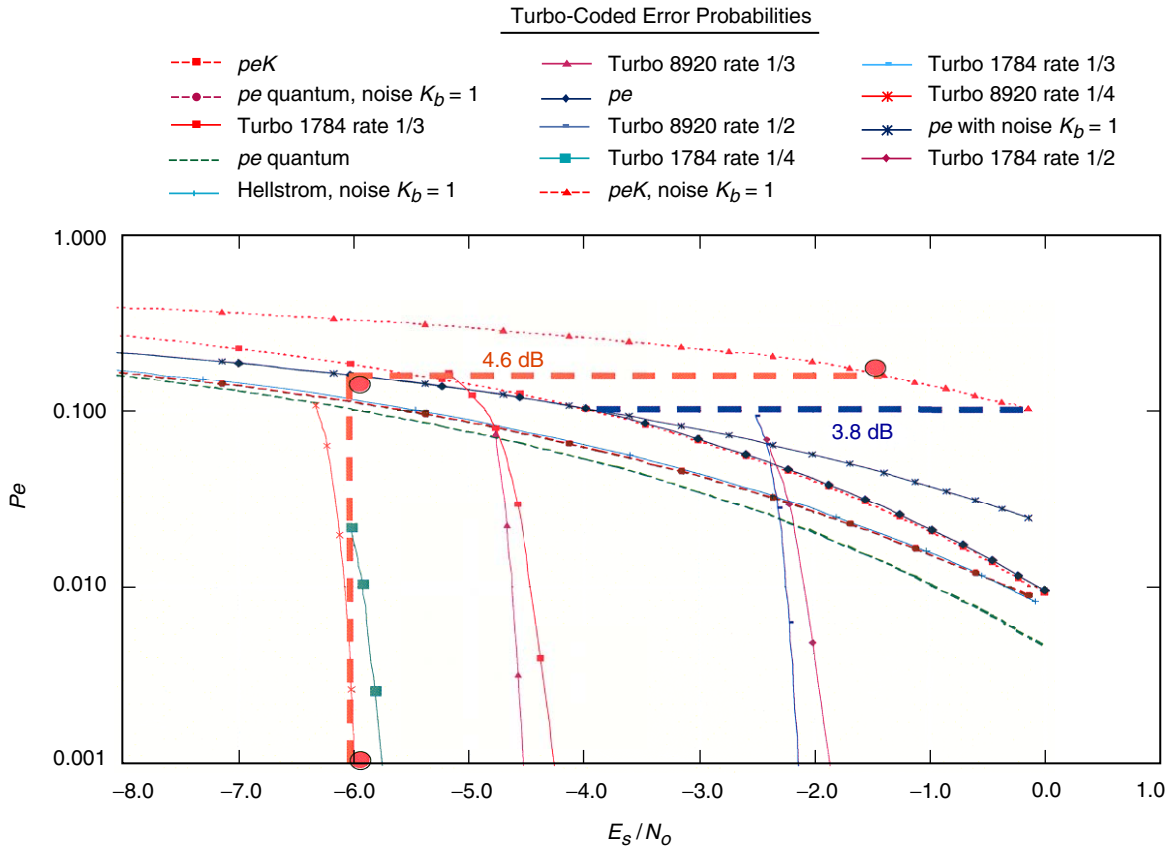

Fig. 6. Coded performance of the vector receiver in the vicinity of the crossover point.

VI. Conclusions

A practical optical receiver structure that employs both the transmitted and reflected components of a realistic optical beam splitter has been examined, and a vector receiver structure that decides on the basis of both outputs has been proposed. Combined field expressions for the two beam-splitter outputs were computed, and the performance of this vector receiver was determined for the case when the near-optimum receiver is assigned to the principal port. Based on practical considerations, coherent detection was proposed and investigated for the auxiliary port, and the performance of the vector receiver was determined for the simplest case of perfect field matching and negligible background photons. It was found that the performance of the vector receiver always improves upon the single-port near-optimum receiver, as expected, when realistic beam-splitter reflectivities are taken into account. However, performance of the vector receiver can be closely approximated by the coherent receiver at the auxiliary port when low signal energies are received, and by the near-optimum receiver at the principal port when the signal energies are high. In the presence of significant background photons, the coherent receiver at the auxiliary port significantly outperforms the noiseless near-optimum receiver at the principal port, and in fact closely approaches the quantum limit for noisy detection. Finally, the impact of coding on vector receiver performance was examined and found to yield greatly improved error probabilities even in the low-photon region of operation.

Acknowledgment

The authors would like to thank Kenneth Andrews for providing the turbo-coded error probabilities in Fig. 6.

References

[1] V. Vilnrotter and C.-W. Lau, "Quantum Detection Theory for the Free-Space Channel," *The Interplanetary Network Progress Report 42-146, April–June 2001*, Jet Propulsion Laboratory, Pasadena, California, pp. 1–34, August 15, 2001. http://ipnpr.jpl.nasa.gov/tmo/progress_report/42-146/146B.pdf

[2] R. S. Kennedy, "A Near-Optimum Receiver for the Binary Coherent State Quantum Channel," *MIT Research Laboratory of Electronics Quarterly Progress Report 108*, Massachusetts Institute of Technology, Cambridge, Massachusetts, pp. 219–225, January 15, 1973.

[3] V. A. Vilnrotter and E. R. Rodemich, "A Generalization of the Near-Optimum Binary Coherent State Receiver Concept," *IEEE Transactions on Information Theory*, vol. IT-30, no. 2, pp. 446–450, March 1984.

[4] S. J. Dolinar, Jr., "An Optimum Receiver for the Binary Coherent State Quantum Channel," *MIT Research Laboratory of Electronics Quarterly Progress Report 111*, Massachusetts Institute of Technology, Cambridge, Massachusetts, pp. 115–120, October 15, 1973.

[5] H. -A. Bachor, *A Guide to Experiments in Quantum Optics*, Weinheim, Germany: Wiley-VCH, 1998.

[6] C. W. Helstrom, J. W. S. Liu, and J. P. Gordon, "Quantum-Mechanical Communication Theory," *Proceedings of the IEEE*, vol. 58, no. 10, pp. 1578–1598, 1970.

[7] C.-W. Lau and V. A. Vilnrotter, "Quantum Detection and Channel Capacity Using State-Space Optimization," *The Interplanetary Network Progress Report 42-148, October–December 2001*, Jet Propulsion Laboratory, Pasadena, California, pp. 1–16, February 15, 2002. http://ipnpr.jpl.nasa.gov/tmo/progress_report/42-148/148G.pdf

[8] V. A. Vilnrotter and C.-W. Lau, "Quantum Detection of Binary and Ternary Signals in the Presence of Thermal Noise Fields," *The Interplanetary Network Progress Report 42-152, October–December 2002*, Jet Propulsion Laboratory, Pasadena, California, pp. 1–13, February 15, 2003. http://ipnpr.jpl.nasa.gov/tmo/progress_report/42-152/152B.pdf